

ALGEBRAIC SYSTEMS BIOLOGY: A CASE STUDY FOR THE WNT PATHWAY

ELIZABETH GROSS, HEATHER A. HARRINGTON, ZVI ROSEN, AND BERND STURMFELS

ABSTRACT. Steady state analysis of dynamical systems for biological networks give rise to algebraic varieties in high-dimensional spaces whose study is of interest in their own right. We demonstrate this for the shuttle model of the Wnt signaling pathway. Here the variety is described by a polynomial system in 19 unknowns and 36 parameters. Current methods from computational algebraic geometry and combinatorics are applied to analyze this model.

1. INTRODUCTION

The theory of biochemical reaction networks is fundamental for systems biology [13, 27]. It is based on a wide range of mathematical fields, including dynamical systems, numerical analysis, optimization, combinatorics, probability, and, last but not least, algebraic geometry. There are numerous articles that use algebraic geometry in the study of biochemical reaction networks, especially those arising from mass action kinetics. A tiny selection is [4, 7, 12, 22, 25].

We here perform a detailed analysis of one specific system, namely the shuttle model for the Wnt signaling pathway, introduced recently by MacLean, Rosen, Byrne, and Harrington [17]. Our aim is twofold: to demonstrate how biology can lead to interesting questions in algebraic geometry and to apply state-of-the-art techniques from computational algebra to biology.

The dynamical system we study consists of the following 19 ordinary differential equations. Their derivation and the relevant background from biology will be presented in Section 2.

$$\begin{aligned}
 \dot{x}_1 &= -k_1x_1 + k_2x_2 \\
 \dot{x}_2 &= k_1x_1 - (k_2 + k_{26})x_2 + k_{27}x_3 - k_3x_2x_4 + (k_4 + k_5)x_{14} \\
 \dot{x}_3 &= k_{26}x_2 - k_{27}x_3 - k_{14}x_3x_6 + (k_{15} + k_{16})x_{15} \\
 \dot{x}_4 &= -k_3x_2x_4 - k_9x_4x_{10} + k_4x_{14} + k_8x_{16} + (k_{10} + k_{11})x_{18} \\
 \dot{x}_5 &= -k_{28}x_5 + k_{29}x_7 - k_6x_5x_8 + k_5x_{14} + k_7x_{16} \\
 \dot{x}_6 &= -k_{14}x_3x_6 - k_{20}x_6x_{11} + k_{15}x_{15} + k_{19}x_{17} + (k_{21} + k_{22})x_{19} \\
 \dot{x}_7 &= k_{28}x_5 - k_{29}x_7 - k_{17}x_7x_9 + k_{16}x_{15} + k_{18}x_{17} \\
 \dot{x}_8 &= -\dot{x}_{16} = -k_6x_5x_8 + (k_7 + k_8)x_{16} \\
 \dot{x}_9 &= -\dot{x}_{17} = -k_{17}x_7x_9 + (k_{18} + k_{19})x_{17} \\
 \dot{x}_{10} &= k_{12} - (k_{13} + k_{30})x_{10} - k_9x_4x_{10} + k_{31}x_{11} + k_{10}x_{18} \\
 \dot{x}_{11} &= -k_{23}x_{11} + k_{30}x_{10} - k_{31}x_{11} - k_{20}x_6x_{11} - k_{24}x_{11}x_{12} + k_{25}x_{13} + k_{21}x_{19} \\
 \dot{x}_{12} &= -\dot{x}_{13} = -k_{24}x_{11}x_{12} + k_{25}x_{13} \\
 \dot{x}_{14} &= k_3x_2x_4 - (k_4 + k_5)x_{14} \\
 \dot{x}_{15} &= k_{14}x_3x_6 - (k_{15} + k_{16})x_{15} \\
 \dot{x}_{18} &= k_9x_4x_{10} - (k_{10} + k_{11})x_{18} \\
 \dot{x}_{19} &= k_{20}x_6x_{11} - (k_{21} + k_{22})x_{19}
 \end{aligned}
 \tag{1}$$

The quantity x_i is a differentiable function of an unknown t , representing time, and $\dot{x}_i(t)$ is the derivative of that function. This dynamical system has five linear conservation laws:

$$(2) \quad \begin{aligned} 0 &= (x_1 + x_2 + x_3 + x_{14} + x_{15}) - c_1 \\ 0 &= (x_4 + x_5 + x_6 + x_7 + x_{14} + x_{15} + x_{16} + x_{17} + x_{18} + x_{19}) - c_2 \\ 0 &= (x_8 + x_{16}) - c_3 \\ 0 &= (x_9 + x_{17}) - c_4 \\ 0 &= (x_{12} + x_{13}) - c_5 \end{aligned}$$

The 31 quantities k_i are the rate constants of the chemical reactions, and the five c_i are the conserved quantities. Both of these are regarded as parameters, so we have 36 parameters in total. Our object of interest is the *steady state variety*, which is the common zero set of the right hand sides of (1) and (2). This variety lives in K^{19} , where K is an algebraically closed field that contains the rational numbers \mathbb{Q} as well as the 36 parameters k_i and c_i . If these parameters are fixed to be particular real numbers then we can take $K = \mathbb{C}$, the field of complex numbers. If it is preferable to regard $\mathbf{k} = (k_1, \dots, k_{31})$ and $\mathbf{c} = (c_1, \dots, c_5)$ as vectors of unknowns, then $K = \overline{\mathbb{Q}(\mathbf{k}, \mathbf{c})}$ is the algebraic closure of the rational function field. In this latter setting, when all parameters are generic, we shall derive the following result:

Theorem 1.1. *The polynomials in (1)–(2) have 9 distinct zeros in K^{19} when $K = \overline{\mathbb{Q}(\mathbf{k}, \mathbf{c})}$.*

By analyzing the steady state variety, we can better understand the model, which is non-linear, and thus the biological system. The aim is to predict the system's behavior, offer biological insight, and determine what data are required to verify or reject the model. Here is a list of questions one might ask about our model from the perspective of systems biology.

Biological Problems. These are labeled according to the section that will address them.

4. *For what real positive rate parameters and conserved quantities does the system exhibit multistationarity?* This question is commonly asked when using a dynamical system for modeling a real-world phenomenon. When modeling a process that experimentally appears to have more than one stable equilibrium, multistationary models are preferred.
5. *Suppose we can measure only a subset of the species concentrations. Which subsets can lead to model rejection?* If all species are measurable at steady state, then we can substitute data into the system (1), and check that all expressions \dot{x}_i are close to zero. If only some x_i are known, we still want to be able to evaluate models with the available data.
6. *Give a complete description of the stoichiometric compatibility classes for the chemical reaction network.* A stoichiometric compatibility class is the set of all points accessible from a given state via the reactions in the system. This question relates more closely to the dynamics of the system, but also has ramifications for the set of all steady states.
7. *What information does species concentration data give us for parameter estimation?* In particular, are the parameters identifiable? Identifiability means that having many measurements of the concentrations \mathbf{x} can determine the reaction rate constants \mathbf{k} . If not identifiable, we will explore algebraic constraints imposed by the species concentration data. This question is relevant for complete and partial steady-state data (usually noisy).

These questions are open challenges for medium to large models in systems biology and medicine [13, 27]. The book chapter [16] illustrates standard mathematical and statistical

methods for addressing these questions, with Wnt signaling as a case study. Here, we examine these questions from the perspective of algebraic geometry. The aim is to provide insight into global behavior by applying tools from nonlinear algebra to synthetic and systems biology. Below are the algebraic problems underlying the four biological problems listed above.

Algebraic Problems.

4. Describe the set of points $(\mathbf{k}, \mathbf{c}) \in \mathbb{R}_{>0}^{31} \times \mathbb{R}_{>0}^5$ such that the polynomials (1)-(2) have two or more positive zeros $\mathbf{x} \in \mathbb{R}_{>0}^{19}$. When is there only one? Identify the discriminant.
5. Which projections of the variety defined by (1) into coordinate subspaces of K^{19} are surjective? Equivalently, describe the algebraic matroid on the ground set $\{x_1, \dots, x_{19}\}$.
6. The conservation relations (2) specify a linear map $\chi : \mathbb{R}^{19} \rightarrow \mathbb{R}^5$, $\mathbf{x} \mapsto \mathbf{c}$. Describe all the convex polyhedra $\chi^{-1}(\mathbf{c}) \cap \mathbb{R}_{\geq 0}^{19}$ where \mathbf{c} runs over the points in the open orthant $\mathbb{R}_{>0}^5$.
7.
 - a. *Complete data*: Describe the matroid on the ground set $\{k_1, k_2, \dots, k_{31}\}$ that is defined by the linear forms on the right hand sides of (1), for fixed steady-state concentrations.
 - b. *Partial steady-state data without noise*: Repeat the analysis after eliminating some of the \mathbf{x} -coordinates.
 - c. *Partial steady-state data with noise*: For the remaining \mathbf{x} -coordinates, suppose that we have data which are *approximately* on the projected steady state variety. Determine a parameter vector (\mathbf{k}, \mathbf{c}) that best fits the data.

In this paper we shall address these questions, and several related ones, after explaining the various ingredients. A particular focus is the exchange between the algebraic formulation and its biological counterpart. Our presentation is organized as follows.

In Section 2 we review the basics on the Wnt signaling pathway, we recall the shuttle model of MacLean *et al.* [17], and we derive the dynamical system (1)–(2). In Section 3 we establish Theorem 1.1, and we examine the set of all steady states. This is here regarded as a complex algebraic variety in an affine space of dimension $55 = 19 + 31 + 5$ with coordinates $(\mathbf{x}, \mathbf{k}, \mathbf{c})$.

In Sections 4, 5, 6, and 7 we address the four problems stated above. The numbers of the problems refer to the respective sections. Each section starts out with an explanation of how the biological problem and the algebraic problem are related. The rationale behind Section 4 is likely to be familiar to most of our readers, given that multistationarity has been discussed widely in the literature; see e.g. [4, 22]. On the other hand, in Section 5 we employ the language of matroid theory. This may be unfamiliar to many readers, especially when it comes to the algebraic matroid associated with an irreducible algebraic variety. Section 6 characterizes the polyhedral geometry encoded in the conservation relations (2). This is a case study in the spirit of [25, Figure 1]. Section 7 addresses the problems of parameter identifiability and parameter estimation. Finally, in Section 8 we return to the biology, and we discuss what our findings might imply for the study of Wnt signaling and other systems.

2. FROM BIOLOGY TO ALGEBRA

Cellular decisions such as cell division, specialization and cell death are governed by a rich repertoire of complex signals that are produced by other cells and/or stimuli. In order for a cell to come to an appropriate decision, it must *sense* its external environment, communicate this information to the nucleus, and respond by regulating genes and producing relevant proteins. Signaling molecules called ligands, external to the cell, can bind to proteins called receptors, initializing the propagation of information within the cell by molecular interactions and modifications (e.g. phosphorylation). This signal may be relayed from the cytoplasm into the nucleus via molecules and the cell responds by activation or deactivation of gene(s) that control, for example, cell fate. The complex interplay of molecules involved in this information transmission is called a signaling transduction pathway. Although many signaling pathways have been defined biochemically, much is still not understood about them or how a signal results in a particular cellular response. Mathematical models constructed at different scales of molecular complexity may help unravel the central mechanisms that govern cellular decisions, and their analysis may inform and guide testable hypotheses and therapies.

In this paper, we focus on the canonical Wnt signaling pathway, which is involved in cellular processes, both during development and in adult tissues. This includes stem cells. Dysfunction of this pathway has been linked to neurodegenerative diseases and cancer. Consequently, Wnt signaling has been widely studied in various organisms, including amphibians and mammals. Researchers are interested in how the extracellular ligand Wnt affects the protein β -catenin, which plays a pivotal role in turning genes on and off in the nucleus.

The molecular interactions within the Wnt signaling pathway are not yet fully understood. This has led to the development and analysis of many mathematical models. The Wnt shuttle model [17] includes an abstraction of the signal transduction pathway (via activation/inactivation of molecules) described above. The model also takes into account molecules that exist, interact and move between different compartments in the cell (e.g., cytoplasm and nucleus). Biologists understand the Wnt system as either *Wnt off* or *Wnt on*. However, such a scenario is rarely binary (i.e., different concentration levels of Wnt may exist) and inherently depends on spatial movement of molecules. The Wnt shuttle model includes complex interactions with nonlinearities arising in the equations. In particular, it includes both the Wnt off and Wnt on scenarios, by adjusting initial conditions or parameter values. The biology needed to understand the model can be described as follows. See also Table 1.

Wnt off: When cells do not sense the extracellular ligand Wnt, β -catenin is degraded (broken down). The degradation of β -catenin is partially dependent on a group of molecules (Axin, APC and GSK-3) that form the *destruction complex*. Crucially, the break down of β -catenin occurs when the destruction complex is in an active state; modification to the destruction complex by proteins, called phosphatases, changes it from inactive to active. Additionally, β -catenin can degrade independent of the destruction complex. Synthesis of β -catenin occurs at a constant rate.

Wnt on: When receptors on the surface of a cell bind to Wnt, the Wnt signaling transduction pathway is initiated. This enables β -catenin to move into the nucleus where it binds with transcription factors that regulate genes. This signal propagation is mediated by the following molecular interactions. After Wnt stimulus, the protein Dishevelled is activated

near the membrane. This in turn inactivates the destruction complex, thereby preventing the destruction of β -catenin, allowing it to accumulate in the cytoplasm through natural synthesis. Throughout the molecular interactions in the signaling pathway, intermediate complexes can form (e.g., β -catenin bound with Dishevelled).

Space: The location of molecules plays a pivotal role: β -catenin moves between the cytoplasm and the nucleus (to reach target genes and regulate them). Dishevelled and molecules that form the destruction complex shuttle between the nucleus and the cytoplasm. However, it is assumed that only the inactive destruction complex can shuttle (since in the cytoplasm it would be bound to β -catenin). Phosphatases exist in both the nucleus and the cytoplasm but the movement across compartments is not included in the model. Symmetry of reactions is assumed if the species exist in both compartments. Intermediate complexes are assumed to be short-lived, or not large enough for movement across compartments.

The Wnt shuttle model of [17] has 19 species whose interactions can be framed as biochemical reactions. These species correspond to variables x_1, \dots, x_{19} in our dynamical system (1). Namely, x_i represents the concentration of the species that is listed in the i th row in Table 1.

Variable	Species	Symbol
	Dishevelled	D
x_1	Dishevelled in cytoplasm (inactive)	D_i
x_2	Dishevelled in cytoplasm (active)	D_a
x_3	Dishevelled in nucleus (active)	D_{an}
	Destruction complex (APC/Axin/GSK3β)	Y
x_4	Destruction complex in cytoplasm (active)	Y_a
x_5	Destruction complex in cytoplasm (inactive)	Y_i
x_6	Destruction complex in nucleus (active)	Y_{an}
x_7	Destruction complex in nucleus (inactive)	Y_{in}
	Phosphatase	P
x_8	Phosphatase in cytoplasm	P
x_9	Phosphatase in nucleus	P_n
	β-catenin	x
x_{10}	β -catenin in cytoplasm	x
x_{11}	β -catenin in nucleus	x_n
	Transcription Factor	T
x_{12}	TCF (gene transcription in nucleus)	T
	Intermediate complex	C
x_{13}	Transcription complex, β -catenin: TCF in nucleus	C_{xT}
x_{14}	Intermediate complex, β -catenin: dishevelled in cytoplasm	C_{YD}
x_{15}	Intermediate complex, destruction complex: dishevelled in nucleus	C_{YDn}
x_{16}	Intermediate complex, destruction complex: phosphatase in cytoplasm	C_{YP}
x_{17}	Intermediate complex, destruction complex: phosphatase in nucleus	C_{YPn}
x_{18}	Intermediate complex, β -catenin: destruction complex in cytoplasm	C_{xY}
x_{19}	Intermediate complex, β -catenin: destruction complex in nucleus	C_{xYn}

Table 1: The 19 species in the Wnt shuttle model.

The second column in Table 1 indicates the biological meaning of the 19 species. The symbols in the last column are those used in the presentation of the Wnt shuttle model in [17].

The 19 species in the model interact according to the 31 reactions given in Table 2. Each reaction comes with a rate constant k_i . These are the coordinates of our parameter vector \mathbf{k} .

Reaction	Explanation
$x_1 \xrightleftharpoons[k_2]{k_1} x_2$	(In)activation of dishevelled, depends on Wnt
$x_2 + x_4 \xrightleftharpoons[k_4]{k_3} x_{14} \xrightarrow{k_5} x_2 + x_5$	Destruction complex active \rightarrow inactive
$x_5 + x_8 \xrightleftharpoons[k_7]{k_6} x_{16} \xrightarrow{k_8} x_4 + x_8$	Destruction complex inactive \rightarrow active
$x_4 + x_{10} \xrightleftharpoons[k_{10}]{k_9} x_{18} \xrightarrow{k_{11}} x_4 + \emptyset$	Destruction complex-dependent β -catenin degradation
$\emptyset \xrightarrow{k_{12}} x_{10}$	β -catenin production
$x_{10} \xrightarrow{k_{13}} \emptyset$	Destruction complex-independent β -catenin degradation
$x_3 + x_6 \xrightleftharpoons[k_{15}]{k_{14}} x_{15} \xrightarrow{k_{16}} x_3 + x_7$	Destruction complex active \rightarrow inactive (nucleus)
$x_7 + x_9 \xrightleftharpoons[k_{18}]{k_{17}} x_{17} \xrightarrow{k_{19}} x_6 + x_9$	Destruction complex inactive \rightarrow active (nucleus)
$x_6 + x_{11} \xrightleftharpoons[k_{21}]{k_{20}} x_{19} \xrightarrow{k_{22}} x_6 + \emptyset$	Destruction complex-dependent β -catenin degradation (nucleus)
$x_{11} \xrightarrow{k_{23}} \emptyset$	Destruction complex-independent β -catenin degradation (nucleus)
$x_{11} + x_{12} \xrightleftharpoons[k_{25}]{k_{24}} x_{13}$	β -catenin binding to TCF (nucleus)
$x_2 \xrightleftharpoons[k_{27}]{k_{26}} x_3$	Shuttling of active dishevelled
$x_5 \xrightleftharpoons[k_{29}]{k_{28}} x_7$	Shuttling of inactive-form destruction complex
$x_{10} \xrightleftharpoons[k_{31}]{k_{30}} x_{11}$	Shuttling of β -catenin

Table 2: The 31 reactions in the Wnt shuttle model.

The 31 reactions in Table 2 translate into a dynamical system $\dot{\mathbf{x}} = \Psi(\mathbf{x}; \mathbf{k})$. Here Ψ is a vector-valued function of the vectors of species concentrations \mathbf{x} and rate constants \mathbf{k} . The choice of Ψ is up to the modeler. In this paper, we assume that Ψ represents the *law of mass action* [13, §2.1.1]. This is precisely what is used in [17] for the Wnt shuttle model. The resulting dynamical system is (1). We refer to [4, 7, 12, 22, 25] and their many references for mass action kinetics and its variants. In summary, Table 2 translates into the dynamical system (1) under the law of mass action. The five relations in (2) constitute a basis for the linear space of conservation relations of the model in Table 2 assuming mass action kinetics.

We refer to x_1, \dots, x_{19} as the *species concentrations*, k_1, \dots, k_{31} as the *rate parameters*, and c_1, \dots, c_5 as the *conserved quantities*. We write \mathbf{x} , \mathbf{k} and \mathbf{c} for the vectors with these coordinates. As is customary in algebraic geometry, we take the coordinates in the complex numbers \mathbb{C} , or possibly in some other algebraically closed field K containing the rationals \mathbb{Q} .

Our aim is to understand the relationships between \mathbf{x} , \mathbf{k} and \mathbf{c} in the Wnt shuttle model. To this end, we introduce the *steady state variety* $\mathcal{S} \subset \mathbb{C}^{55}$. This is the set of all points $(\mathbf{x}, \mathbf{k}, \mathbf{c})$ that satisfy the equations $\dot{x}_1 = \dots = \dot{x}_{19} = 0$ in (1) along with the five conservation laws in (2). We write our ambient affine space as $\mathbb{C}^{55} = \mathbb{C}_{\mathbf{x}}^{19} \times \mathbb{C}_{\mathbf{k}}^{31} \times \mathbb{C}_{\mathbf{c}}^5$. This emphasizes the distinction between the species concentrations, rate parameters, and conserved quantities.

3. IDEALS, VARIETIES, AND NINE POINTS

We write I for the ideal in the polynomial ring $\mathbb{Q}[\mathbf{x}, \mathbf{k}] = \mathbb{Q}[x_1, \dots, x_{19}, k_1, \dots, k_{31}]$ that is generated by the 19 polynomials \dot{x}_i on the right hand side of (1). Five of these generators are redundant. Indeed, the conservation relations (2) give the following identities modulo I :

$$\begin{aligned} \dot{x}_1 + \dot{x}_2 + \dot{x}_3 + \dot{x}_{14} + \dot{x}_{15} &= \dot{x}_8 + \dot{x}_{16} = \dot{x}_9 + \dot{x}_{17} = \dot{x}_{12} + \dot{x}_{13} = \\ \dot{x}_4 + \dot{x}_5 + \dot{x}_6 + \dot{x}_7 + \dot{x}_{14} + \dot{x}_{15} + \dot{x}_{16} + \dot{x}_{17} + \dot{x}_{18} + \dot{x}_{19} &= 0. \end{aligned}$$

For instance, the polynomials \dot{x}_{13} , \dot{x}_{15} , \dot{x}_{16} , \dot{x}_{17} and \dot{x}_{19} are redundant because they can be expressed as negated sums of other generators of I . Hence I is generated by 14 polynomials. The variety $V(I)$ lives in the 50-dimensional affine space $\mathbb{C}_{\mathbf{x}}^{19} \times \mathbb{C}_{\mathbf{k}}^{31}$, and it is isomorphic to the steady state variety $\mathcal{S} \subset \mathbb{C}^{55}$. A direct computation using the computer algebra package `Macaulay2` [11] shows that $V(I)$ has dimension 36. Hence the affine ideal I is a complete intersection in $\mathbb{Q}[\mathbf{x}, \mathbf{k}]$. Furthermore, using `Macaulay2` we can verify the following lemma.

Lemma 3.1. *The ideal I admits the non-trivial decomposition $I = I_m \cap I_e$, where $I_e = I : \langle x_1 \rangle$ and $I_m = I + \langle x_1 \rangle$, both of these components have codimension 14, and I_e is a prime ideal.*

The ideal I_m is called the *main component*, while I_e is called the *extinction component*, since it reflects those steady states where a number of the reactants “run out.” Both of these ideals live in $\mathbb{Q}[\mathbf{x}, \mathbf{k}]$, and we now present explicit generators. The extinction component equals

$$\begin{aligned} I_e = \langle &x_1, x_2, x_3, x_5, x_7, x_{14}, x_{15}, x_{16}, x_{17}, k_{30}x_{10} - (k_{23} + k_{31})x_{11} - k_{22}x_{19}, \\ &k_{13}x_{10} + k_{23}x_{11} + k_{11}x_{18} + k_{22}x_{19} - k_{12}, k_{24}x_{11}x_{12} - k_{25}x_{13}, \\ &k_{20}x_6x_{11} - (k_{21} + k_{22})x_{19}, k_9x_4x_{10} - (k_{10} + k_{11})x_{18} \rangle. \end{aligned}$$

The ideal I_e is found to be prime in $\mathbb{Q}[\mathbf{x}, \mathbf{k}]$. The main component equals

$$\begin{aligned} I_m = \langle &k_{16}x_{15} - k_{19}x_{17}, k_5x_{14} - k_8x_{16}, k_{30}x_{10} - (k_{23} + k_{31})x_{11} - k_{22}x_{19}, \\ &k_{13}x_{10} + k_{23}x_{11} + k_{11}x_{18} + k_{22}x_{19} - k_{12}, k_{28}x_5 - k_{29}x_7, k_{26}x_2 - k_{27}x_3, \\ &k_1x_1 - k_2x_2, k_{24}x_{11}x_{12} - k_{25}x_{13}, k_{20}x_6x_{11} - (k_{21} + k_{22})x_{19}, \\ &k_9x_4x_{10} - (k_{10} + k_{11})x_{18}, k_{17}x_7x_9 - (k_{18} + k_{19})x_{17}, k_6x_5x_8 - (k_7 + k_8)x_{16}, \\ &k_{14}x_3x_6 - k_{15}x_{15} - k_{19}x_{17}, k_3x_2x_4 - k_4x_{14} - k_8x_{16}, \\ &(k_4k_6k_8k_{14}k_{16}k_{18}k_{26}k_{29} + k_5k_6k_8k_{14}k_{16}k_{18}k_{26}k_{29} + \\ &k_4k_6k_8k_{14}k_{16}k_{19}k_{26}k_{29} + k_5k_6k_8k_{14}k_{16}k_{19}k_{26}k_{29})k_1x_6x_8 \\ &- (k_3k_5k_7k_{15}k_{17}k_{19}k_{27}k_{28} + k_3k_5k_8k_{15}k_{17}k_{19}k_{27}k_{28} \\ &+ k_3k_5k_7k_{16}k_{17}k_{19}k_{27}k_{28} + k_3k_5k_8k_{16}k_{17}k_{19}k_{27}k_{28})k_1x_4x_9 \rangle. \end{aligned}$$

This ideal is not prime in $\mathbb{Q}[\mathbf{x}, \mathbf{k}]$. For instance, the variable k_1 is a zerodivisor modulo I_m , as seen from the last generator. Removing the factor k_1 from the last generator yields the quotient ideal $I_m : \langle k_1 \rangle$. However, even that ideal still has several associated primes. All of these prime ideals, except for one, contain some of the rate constants k_i .

That special component is characterized in the following proposition. Given any ideal $J \subset \mathbb{Q}[\mathbf{x}, \mathbf{k}]$, we write $\widetilde{J} = \mathbb{Q}(\mathbf{k})[\mathbf{x}]J$ for its extension to the polynomial ring $\mathbb{Q}(\mathbf{k})[\mathbf{x}]$ in the unknowns x_1, \dots, x_{19} over the field of rational functions in the parameters k_1, \dots, k_{31} .

Proposition 3.2. *The ideal $J_m = \widetilde{I}_m \cap \mathbb{Q}[\mathbf{x}, \mathbf{k}]$ is prime. Its irreducible variety $V(J_m) \subset \mathbb{C}^{50}$ has dimension 36; it is the unique component of $V(I_m)$ that maps dominantly onto $\mathbb{C}_{\mathbf{k}}^{31}$.*

Proof. The ideal \widetilde{I}_m has the same generators as I_m but now regarded as polynomials in \mathbf{x} with coefficients in $\mathbb{Q}(\mathbf{k})$. Symbolic computation in the ring $\mathbb{Q}(\mathbf{k})[\mathbf{x}]$ reveals that \widetilde{I}_m is a prime ideal. This implies that J_m is a prime ideal in $\mathbb{Q}[\mathbf{x}, \mathbf{k}]$, and hence $V(J_m)$ is irreducible. The dimension statement follows from the result of Lemma 3.1 that I_m is a complete intersection. This ensures that $V(I_m)$ has no lower-dimensional components, by Krull's Principal Ideal Theorem. Finally, $V(J_m)$ maps dominantly onto $\mathbb{C}_{\mathbf{k}}^{31}$ because $J_m \cap \mathbb{Q}[\mathbf{k}] = \{0\}$. \square

Corollary 3.3. *The ideal \widetilde{I} is radical, and it is the intersection of two primes in $\mathbb{Q}(\mathbf{k})[\mathbf{x}]$:*

$$(3) \quad \widetilde{I} = \widetilde{I}_e \cap \widetilde{I}_m.$$

Proof. This follows directly from Proposition 3.2 and the primality of I_e in Lemma 3.1. \square

The decomposition has the following geometric interpretation. We now work over the field $K = \overline{\mathbb{Q}(\mathbf{k})}$. All rate constants are taken to be generic. Then $V(\widetilde{I})$ is the 5-dimensional variety of all steady states in K^{19} . This variety is the union of two irreducible components,

$$V(\widetilde{I}) = V(\widetilde{I}_e) \cup V(\widetilde{I}_m),$$

where each component is 5-dimensional. The first component lies inside the 10-dimensional coordinate subspace $V(x_1, x_2, x_3, x_5, x_7, x_{14}, x_{15}, x_{16}, x_{17})$. Hence it is disjoint from the hyperplane defined by the first conservation relation $x_1 + x_2 + x_3 + x_{14} + x_{15} = c_1$. In other words, $V(\widetilde{I}_e)$ is mapped into a coordinate hyperplane under the map $\chi : K^{19} \rightarrow K^5, \mathbf{x} \mapsto \mathbf{c}$.

On the other hand, the second component $V(\widetilde{I}_m)$ maps dominantly onto K^5 under χ . Theorem 1.1 states that the generic fiber of this map consists of 9 reduced points. Equivalently,

$$(4) \quad \chi^{-1}(\mathbf{c}) \cap V(\widetilde{I}) = \chi^{-1}(\mathbf{c}) \cap V(\widetilde{I}_m)$$

is a set of nine points in K^{19} . We are now prepared to argue that this is indeed the case.

Computational Proof of Theorem 1.1. We consider the ideal of the variety (4) in the polynomial ring $\mathbb{Q}(\mathbf{k}, \mathbf{c})[\mathbf{x}]$. This polynomial ring has 19 variables, and all 36 parameters are now scalars in the coefficient field. This ideal is generated by the right hand sides of (1) and (2). Performing a Gröbner basis computation in this polynomial ring verifies that our ideal is zero-dimensional and has length 9. Hence (4) is a reduced affine scheme of length 9 in K^{19} .

Fast numerical verification of this result is obtained by replacing the coordinates of \mathbf{k} and \mathbf{c} with generic (random rational) values. In `Macaulay2` one finds, with probability 1, that the

resulting ideals in $\mathbb{Q}[\mathbf{x}]$ are radical of length 9. We also verified this result via *numerical algebraic geometry*, using the two software packages **Bertini** [1] and **PHCpack** [26]. \square

4. MULTISTATIONARITY AND ITS DISCRIMINANT

This section centers around Question 4 from the Introduction: *For what real positive rate parameters and conserved quantities does the system exhibit multistationarity?* This is commonly asked about biochemical reaction networks and about dynamical systems in general.

Mathematically, this is a problem of *real algebraic geometry*. Writing \mathcal{S} for the steady state variety in \mathbb{C}^{55} , we are interested in the fibers of the map $\pi_{\mathbf{k},\mathbf{c}} : \mathcal{S} \cap \mathbb{R}_{>0}^{55} \rightarrow \mathbb{R}_{>0,\mathbf{k}}^{31} \times \mathbb{R}_{>0,\mathbf{c}}^5$. According to Theorem 1.1, the general fiber consists of 9 *complex* points $\mathbf{x} \in \mathbb{C}_{\mathbf{x}}^{19}$, when the map $\pi_{\mathbf{k},\mathbf{c}}$ is taken over \mathbb{C} . But here we take it over the reals \mathbb{R} or over the positive reals $\mathbb{R}_{>0}$.

In our application to biology, we only care about concentration vectors \mathbf{x} whose coordinates are real and positive. Thus we wish to stratify $\mathbb{R}_{>0,\mathbf{k}}^{31} \times \mathbb{R}_{>0,\mathbf{c}}^5$ according to the cardinality of

$$(5) \quad \pi_{\mathbf{k},\mathbf{c}}^{-1}(\mathbf{k}, \mathbf{c}) = \{ (\mathbf{x}, \mathbf{k}', \mathbf{c}') \in \mathcal{S} \cap \mathbb{R}_{>0}^{55} : \mathbf{k}' = \mathbf{k} \text{ and } \mathbf{c}' = \mathbf{c} \}.$$

This stratification comes from a decomposition of the 36-dimensional orthant $\mathbb{R}_{>0,\mathbf{k}}^{31} \times \mathbb{R}_{>0,\mathbf{c}}^5$ into connected open semialgebraic subsets. The walls in this decomposition are given by the *discriminant* Δ , a giant polynomial in the 36 unknowns (\mathbf{k}, \mathbf{c}) that is to be defined later.

We begin with the following result on what is possible with regard to real positive solutions.

Theorem 4.1. *Consider the polynomial system in (1)–(2) where all parameters k_i and c_j are positive real numbers. The set (5) of positive real solutions can have 1, 2, or 3 elements.*

Proof. For random choices of $(\mathbf{k}, \mathbf{c}) = (k_1, \dots, k_{31}, c_1, \dots, c_5)$ in the orthant $\mathbb{R}_{>0}^{36}$, our polynomial system has 9 complex solutions, by Theorem 1.1. For the following two special choices of the 36 parameter values, all 9 solutions are real. First, take (\mathbf{k}, \mathbf{c}) to be the vector

$$(1.7182818, 53.2659, 3.4134082, 0.61409879, 0.61409879, 3.4134082, 0.98168436, 0.98168436, \\ 92.331732, 0.86466471, 79.9512906, 97.932525, 1, 3.2654672, 0.61699064, 0.61699064, \\ 37.913879, 0.86466471, 0.86466471, 4.7267833, 0.17182818, 0.68292191, 1, 0.55950727, \\ 1.0117639, 1.7182818, 1.7182818, 0.99326205, 0.99326205, 5.9744464, 1, 4.9951026, \\ 16.4733784, 1.6006340000000001, 1.2089126, 2.7756596399999998).$$

The resulting system has three positive solutions $\mathbf{x} \in \mathbb{R}_{>0}^{19}$. Next, let $(\mathbf{k}', \mathbf{c}')$ be the vector

$$(0.948166, 7.45086, 5.72974, 3.96947, 7.21145, 7.8761, 1.87614, 8.11372, 6.21862, 5.24801, \\ 3.10707, 1.08146, 5.22133, 5.84158, .911392, 4.28788, 4.81201, 9.67849, 1.34452, 7.38597, \\ 6.64451, 7.10229, 8.57942, 5.79076, 6.33244, 1.53916, 1.39658, 0.81673, 5.8434, 3.86223, \\ 7.22696, 1.45438, 3.36482, 6.06453, 4.82045, 3.6014).$$

Here, one solution to our system is positive. By connecting the two parameter points above with a general curve in $\mathbb{R}_{>0}^{36}$, and by examining in-between points $(\mathbf{k}'', \mathbf{c}'')$, we can construct a system with two positive solutions. All computations were carried out using **Bertini** [1]. \square

Remark 4.2. At present, we do not know whether the number of real positive solutions can be larger than three. We suspect that this is impossible, but we currently cannot prove it.

The difficulty lies in the fact that the stratification of $\mathbb{R}_{>0}^{36}$ is extremely complicated. In computer algebra, the derivation of such stratifications is known as the problem of *real root classification*. For a sample of recent studies in this direction see [3, 6, 23]. Real root classification is challenging even when the number of parameters is 3 or 4; clearly, 36 parameters is out of the question. The stratification of $\mathbb{R}_{>0}^{36}$ by behavior of (5) has way too many cells.

While symbolic techniques for real root classification are infeasible for our system, we can use numerical algebraic geometry [9] to gain insight into the stratification of $\mathbb{R}_{>0}^{36}$. *Coefficient-parameter homotopies* [19] can solve the steady state polynomial system (1)-(2) for multiple choices of (\mathbf{k}, \mathbf{c}) quickly. For our computations we use `Bertini.m2`. This is the Bertini interface for `Macaulay2`, as described in [2]. Each system has 19 equations in 19 unknowns and, for random (\mathbf{k}, \mathbf{c}) , each system has 9 complex solutions. Such a system can be solved in less than one second using the `bertiniParameterHomotopy` function from `Bertini.m2`.

Below we describe the following experiment. We sample 10,000 parameter vectors (\mathbf{k}, \mathbf{c}) from two different probability distributions on $\mathbb{R}_{>0}^{36}$. In each case we report the observed frequencies for the number of real solutions and number of positive solutions. We then follow these experiments with a specialized sampling scheme for testing numerical robustness.

Uniform sampling scheme: Here we choose (\mathbf{k}, \mathbf{c}) uniformly from the cube $(0.0, 100.0)^{36}$. Sampling 10,000 parameter vectors from this scheme and solving the steady state system for each of these parameter vectors in `Bertini`, we obtained 9,992 solutions sets that contained 9 complex points. Solution sets with less than 9 points occur when some paths in the coefficient-parameter homotopy fail. We call solution sets with 9 solutions *good*.

Integer sampling scheme: Here we select (\mathbf{k}, \mathbf{c}) uniformly from $\{1, 2, 3\}^{36}$. Sampling 10,000 parameter vectors according to this scheme and solving the corresponding steady state system returned 9,963 good solution sets. Below is a table that records how many of the good solution sets had 9, 7, 5, 3 real solutions; all solution sets had 1 positive real solution.

# of real solutions	9	7	5	3
Freq. for Uniform Sampling	5,760	3,675	544	13
Freq. for Integer Sampling	2,138	5,181	2,522	122

Table 3: Frequencies for the sampling schemes.

These computations indicate that for most parameter vectors in $(0, 100)^{36}$ we will see only one positive solution to the steady state system. But while the set of parameter vectors that result in multiple steady states is not very large, we can give evidence that multistationarity is preserved under small perturbations. This is our next point.

Testing Robustness: Let $(\mathbf{k}^*, \mathbf{c}^*)$ be the first point in the proof of Theorem 4.1. For each index $i \in \{1, \dots, 19\}$ we choose y_i uniformly from $(-0.03 \cdot k_i^*, 0.03 \cdot k_i^*)$ then set $k_i = k_i^* + y_i$. We ran the same process for the c_i . Sampling 10,000 parameter vectors this way and solving the corresponding steady state systems returned 10,000 good solution sets, as follows:

# of real solutions	Freq.	# of pos. solutions	Freq.
9	9,879	3	9,879
7	121	1	121

Table 4: Frequencies for testing robustness scheme.

In the remainder of this section, we properly define the discriminant Δ that separates the various strata in $\mathbb{R}_{>0}^{36}$. Let Δ_{int} denote the Zariski closure in $\mathbb{C}_{\mathbf{k}}^{31} \times \mathbb{C}_{\mathbf{c}}^5$ of all parameter vectors (\mathbf{k}, \mathbf{c}) for which (1)–(2) does not have 9 isolated complex solutions and there are no solutions with $x_i = 0$ for some i . It can be shown that Δ_{int} is a hypersurface that is defined over \mathbb{Q} , so it is given by a unique (up to sign) irreducible squarefree polynomial in $\mathbb{Z}[\mathbf{k}, \mathbf{c}]$. We use the symbol Δ_{int} also for that polynomial. To be precise, Δ_{int} is the discriminant of a number field L with $K \supset L \supset \mathbb{Q}$, namely L is the field of definition of the finite K -scheme (4).

Next, for any $i \in \{1, 2, \dots, 19\}$ consider the intersection of the steady state variety \mathcal{S} with the hyperplane $\{x_i = 0\}$. The Zariski closure of the image of $\mathcal{S} \cap \{x_i = 0\}$ under the map $\pi_{\mathbf{k}, \mathbf{c}}$ is a hypersurface in $\mathbb{C}_{\mathbf{k}}^{19} \times \mathbb{C}_{\mathbf{c}}^{31}$, defined over \mathbb{Q} , and we write $\Delta_{x_i=0}$ for the unique (up to sign) irreducible polynomial in $\mathbb{Z}[\mathbf{k}, \mathbf{c}]$ that vanishes on that hypersurface. We now define

$$\Delta := \Delta_{\text{int}} \cdot \text{lcm}(\Delta_{x_1=0}, \Delta_{x_2=0}, \dots, \Delta_{x_{19}=0}).$$

This product with a least common multiple (lcm) is the *discriminant* for our problem.

Example 4.3. The degree of Δ_{int} as a polynomial only in $\mathbf{c} = (c_1, c_2, c_3, c_4, c_5)$ equals 34. To illustrate this, we set $\mathbf{c} = (5, 16 + C, \frac{8}{5} - C, \frac{6}{5} + C, 3 - C)$ where C is a parameter, and

$$\mathbf{k} = \left(\frac{9}{5}, \frac{9}{5}, 3, \frac{2}{3}, \frac{2}{3}, 3, 1, 1, 100, \frac{4}{5}, 80, 100, 1, 3, \frac{2}{3}, \frac{2}{3}, 38, \frac{4}{5}, \frac{4}{5}, 4, \frac{1}{8}, \frac{3}{5}, 1, \frac{1}{2}, 19, \frac{7}{4}, \frac{7}{4}, 1, 1, 5, 1 \right).$$

Under this specialization, the polynomial Δ_{int} becomes an irreducible polynomial of degree 34 in the parameter C . Its coefficients are enormously large integers. It has 14 real roots.

For the other factors $\Delta_{x_i=0}$ of the discriminant, we find the following specializations:

$$(6) \quad \begin{aligned} x_1 &\rightarrow 0, & x_2 &\rightarrow 0, & x_3 &\rightarrow 0, & x_4 &\rightarrow (C+16)(5C-8), & x_5 &\rightarrow C+16, & x_6 &\rightarrow (C+16)(5C+6), \\ x_7 &\rightarrow C+16, & x_8 &\rightarrow 5C-8, & x_9 &\rightarrow 5C+6, & x_{10} &\rightarrow \text{a quartic } q(C), & x_{11} &\rightarrow 0, & x_{12} &\rightarrow C-3, \\ x_{13} &\rightarrow C-3, & x_{14} &\rightarrow (C+16)(5C-8), & x_{15} &\rightarrow (C+16)(5C+6), & x_{16} &\rightarrow (C+16)(5C-8), \\ & & x_{17} &\rightarrow (C+16)(5C+6), & x_{18} &\rightarrow (C+16)(5C-8)q(C), & x_{19} &\rightarrow (C+16)(5C+6). \end{aligned}$$

These polynomials have 8 distinct real roots in total, so the total number of real roots of the discriminant is $14 + 8 = 22$. These are the break points where real root behavior changes:

(9, 0)	-77.2388	(9, 0)	-16.0000	(9, 0)	-5.28669	(7, 0)	-1.57472
(9, 0)	-1.46506	(9, 0)	-1.34899	(7, 0)	-1.29581	(9, 0)	-1.20000
(9, 1)	-1.19215	(9, 1)	-1.18389	(7, 1)	-0.584325	(9, 3)	-0.361808
(7, 3)	0.191039	(5, 1)	1.30812	(7, 1)	1.33197	(5, 1)	1.60000
(5, 0)	1.60161	(3, 0)	3.0000	(3, 0)	4.26306	(5, 0)	11.1174
(7, 0)	21.4165	(9, 0)	310.141	(9, 0)			

In this table, we list all 22 roots of the specialized discriminant $\Delta(C)$. The eight boldface values of C are the roots of (6): here one of the coordinates of \mathbf{x} becomes zero. At the other 14 values of C , the number of real roots changes. Between any two roots we list the pair (r, p) , where r is the number of real roots and p is the number of positive real roots. For instance, for $-0.361808 < C < 0.191039$, there are 7 real roots of which 3 are positive.

5. ALGEBRAIC MATROIDS AND PARAMETRIZATIONS

Question 5 asks: *Suppose we can measure only a subset of the species concentrations. Which subsets can lead to model rejection?* This issue is important for the Wnt shuttle model because, in the laboratory, only some of the species are measurable by existing techniques.

We shall address Question 5 using *algebraic matroids*. Matroid theory allows us to analyze the structure of relationships among the 19 species in Table 1. This first appeared in [17]. We here present an in-depth study of the matroids that govern the Wnt shuttle model.

An introduction to (algebraic) matroids can be found in [21]; they have been applied in [14, 15] to problems involving the completion of partial information. General algorithms for computing algebraic matroids are derived in [24]. We briefly review basic notions.

Definition 5.1. A *matroid* is an ordered pair (X, \mathcal{I}) , where X is a finite set, here regarded as unknowns, and \mathcal{I} is a subset of the power set of X . These satisfy certain *independence axioms*. For an *algebraic matroid*, we are given a prime ideal P in the polynomial ring $K[X]$ generated by X , and \mathcal{I} consists of subsets of X whose images in $K[X]/P$ are algebraically independent over K . Thus, the collection of independent sets is $\mathcal{I} = \{Y \subseteq X : P \cap K[Y] = \{0\}\}$.

1. *Bases* are maximal independent sets, i.e. subsets in \mathcal{I} that have maximal cardinality.
2. *Rank* is a function ρ from the power set of X to the natural numbers, which takes as input a set $Y \subset X$ and returns the cardinality of the largest subset of Y in \mathcal{I} .
3. *Closure* is a function from the power set 2^X to itself. The input is a set Y and the output is the largest set containing Y with the same rank.
4. *Flats* are the elements in 2^X that lie in the image of the closure map.
5. *Circuits* are the sets of minimal cardinality **not** contained in \mathcal{I} .

We are here interested in the matroid that is defined by the prime ideal $P = \widetilde{I}_m$ in $\mathbb{Q}(\mathbf{k})[\mathbf{x}]$. Its ground set X is the set of species concentrations $\{x_1, \dots, x_{19}\}$. Since $V(\widetilde{I}_m)$ is 5-dimensional, each basis consists of five elements in X . In our application, bases are the maximal subsets of X that can be specified independently at steady state; they are also the minimal-cardinality sets that can be measured to learn all species concentrations. The rank of a set Y indicates the number of measurements required to learn the concentrations for every element of Y . Flats are the full subsets that are specified by any given collection of measurements.

Circuits furnish our answer to Question 5: they are minimal sets of species that can be used to test compatibility of the data with the model. For each circuit Y there is a unique up-to-scalars relation in $\widetilde{I}_m \cap \mathbb{Q}(\mathbf{k})[Y]$, called the *circuit polynomial* of Y . If the measurements indicate that this relation is not satisfied, then the model and data are not compatible.

Proposition 5.2. *The algebraic matroid of \widetilde{I}_m has rank 5. It has 951 circuits, summarized in Table 5. Of the 11628 subsets of X of size 5, precisely 2389 are bases. The 2092 bases summarized in Table 6 have base degree 1, while the remaining 297 have base degree 2.*

The computation of this matroid was carried out using the methods described in [24]. It was first reported in [17], along with the matroids of alternative models for the Wnt pathway. The idea there was to find subsets of variables that were dependent for different models.

Our matroid analysis here goes beyond [17] in several ways:

1. We keep track of the parameters \mathbf{k} . We take our circuit polynomials to have (relatively prime) coefficients in $\mathbb{Z}[\mathbf{k}]$. This gives us a new tool for model rejection, e.g. in situations where only one data point is known but some parameter values are available.
2. We show how circuits can be used in parameter estimation; this will be done in Section 8.
3. We use the degree-1 bases to derive rational parametrizations of the variety $V(\widetilde{I}_m)$.

We now explain Table 5. A circuit polynomial has *type* (i, j) if it contains i species concentrations (\mathbf{x} -variables) and j rate parameters (\mathbf{k} -variables). The entry in row i and column j in Table 5 is the number of circuits of type (i, j) . Zero values are omitted for clarity.

	2	3	4	5	6		2	3	4	5	6		2	3	4	5	6
2	5	1				12			13	10		22			8	58	
3		6				13			13	15	2	23			4	56	5
4	1	5				14			19	16	1	24				54	14
5		6	1			15			17	21	4	25				53	15
6		7	5			16			15	11	2	26				8	16
7		5	3			17			16	32	9	27			12	56	16
8		1	11	1		18			4	6	2	28			2		2
9		6	12	3		19			26	36	11	29				29	14
10			11	1		20			44	1	1	30					
11		4	7	11	1	21			26	27	9	31					6

TABLE 5. The 951 circuit polynomials, by numbers of unknowns x_i and k_j .

Example 5.3. There are five circuits of type $(2, 2)$. One of them is $\dot{x}_1 = -k_1x_1 + k_2x_2$. Most of the 951 circuit polynomials in \widetilde{I}_m are more complicated. In particular, they are non-linear in both \mathbf{x} and \mathbf{y} . For instance, the unique circuit polynomial of type $(6, 11)$ equals

$$\begin{aligned} & (-k_{15}k_{17}k_{19}k_{20}k_{25} - k_{16}k_{17}k_{19}k_{20}k_{25})x_7x_9x_{13} \\ & + (k_{14}k_{16}k_{18}k_{21}k_{24} + k_{14}k_{16}k_{19}k_{21}k_{24} + k_{14}k_{16}k_{18}k_{22}k_{24} + k_{14}k_{16}k_{19}k_{22}k_{24})x_3x_{12}x_{19}. \end{aligned}$$

In Section 7, we will consider the role of these nonlinear functions in parameter estimation.

Given a basis Y of an algebraic matroid, its *base degree* is the length of the generic fiber of the projection of $V(P)$ onto the Y -coordinates (cf. [24]). Bases with degree 1 are desirable:

Proposition 5.4. *Let $P \subset K[X]$ be a prime ideal, Y a basis of its algebraic matroid, $|X| = n$, and $|Y| = r$. If Y has base degree 1 then $V(P)$ is a rational variety, and the basic circuits of Y specify a birational map $\varphi_Y : K^r \dashrightarrow K^n$ whose image is Zariski dense in $V(P)$*

Proof. For each coordinate x_i in $X \setminus Y$ there exists a circuit containing $Y \cup \{x_i\}$; this is the *basic circuit* of (Y, x_i) . Since Y has base degree 1, the generic fiber of the map $V(P) \rightarrow K^r$ consists of a unique point. Therefore the circuit polynomial is linear in x_i . It has the form

$$p_i(Y) \cdot x_i + q_i(Y), \quad \text{where } p_i, q_i \in K[Y].$$

The i -coordinate of the rational map φ_Y equals x_i if $x_i \in Y$ and $-q_i(Y)/p_i(Y)$ if $x_i \notin Y$. \square

From Propositions 5.2 and 5.4, we obtain 2092 rational parametrizations of the variety $V(\widetilde{I}_m)$. These are the maps $\varphi_Y : K^5 \dashrightarrow K^{19}$, where Y runs over all bases of base degree 1. Using these φ_Y , we obtain 2092 representations of the steady state variety (4) as a subset of K^5 , where now $K = \mathbb{Q}(\mathbf{k}, \mathbf{c})$. Namely, we consider the preimages of the five hyperplanes defined by (2). These are hypersurfaces in K^5 whose intersection represents the nine points in (4). We performed the following computation for all 2092 bases $Y = \{y_1, \dots, y_5\}$ of base degree 1:

1. Substitute $\mathbf{x} = \varphi_Y(y_1, \dots, y_5)$ into the five linear equations (2).
2. Clear the denominators d_1, \dots, d_5 in each equation to get polynomials h_1, \dots, h_5 in Y .
3. The saturation ideal $J_Y = \langle h_1, \dots, h_5 \rangle : \langle d_1 d_2 \cdots d_5 \rangle^\infty$ represents the preimage of (4).

Given such a wealth of parametrizations, we seek one where J_Y has desirable properties. We use the following criterion: consider subsets of five of the generators of J_Y , compute the *mixed volume* of their Newton polytopes, and fix a subset minimizing that mixed volume. In the census of 2092 bases in Table 6, that minimum is referred to as the mixed volume of Y .

<i>Mixed Volume</i>	5	9	10	11	12	13	14	15	16	20	23	24	25	30	35	42	45
<i>Frequency</i>	2	416	6	73	50	167	563	751	10	12	6	1	11	12	4	4	4

TABLE 6. Reducing the steady state equations to the 2092 bases of base degree 1

By Bernstein's Theorem, the mixed volume is the number of solutions to a generic system with the five given Newton polytopes. We seek bases Y where this matches the number nine from Theorem 1.1. We see that the mixed volume is nine for 416 of the bases, in Table 6.

Example 5.5. The basis $Y = \{x_1, x_4, x_6, x_8, x_{13}\}$ has base degree 1 and mixed volume 9. The remaining variables can be expressed in terms of Y as follows. For brevity, we set

$$r(x_4, x_6) = k_9 k_{11} k_{20} k_{22} x_4 x_6 + k_9 k_{11} (k_{21} + k_{22}) (k_{23} + k_{31}) x_4 + k_{20} k_{22} (k_{10} + k_{11}) (k_{13} + k_{30}) x_6 + (k_{10} + k_{11}) (k_{21} + k_{22}) (k_{13} k_{23} + k_{23} k_{30} + k_{13} k_{31}).$$

$x_2 = \frac{k_1}{k_2} x_1$	$x_{12} = \frac{r(x_4, x_6)}{k_{12} k_{30} (k_{10} + k_{11}) (k_{21} + k_{22})} \frac{k_{25}}{k_{24}} x_{13}$
$x_3 = \frac{k_1 k_{26}}{k_2 k_{27}} x_1$	$x_{14} = \frac{k_1 k_3}{k_2 (k_4 + k_5)} x_1 x_4$
$x_5 = \frac{k_1 k_3 k_5 (k_7 + k_8)}{k_2 k_6 k_8 (k_4 + k_5)} \frac{x_1 x_4}{x_8}$	$x_{15} = \frac{k_1 k_{14} k_{26}}{k_2 k_{27} (k_{15} + k_{16})} x_1 x_6$
$x_7 = \frac{k_1 k_3 k_5 k_{28} (k_7 + k_8)}{k_2 k_6 k_8 k_{29} (k_4 + k_5)} \frac{x_1 x_4}{x_8}$	$x_{16} = \frac{k_1 k_3 k_5}{k_2 k_8 (k_4 + k_5)} x_1 x_4$
$x_9 = \frac{k_6 k_8 k_{14} k_{16} k_{26} k_{29} (k_4 + k_5) (k_{18} + k_{19})}{k_3 k_4 k_5 k_{17} k_{19} k_{27} k_{28} (k_7 + k_8) (k_{15} + k_{16})} \frac{x_6 x_8}{x_4}$	$x_{17} = \frac{k_1 k_{14} k_{16} k_{26}}{k_2 k_{19} k_{27} (k_{15} + k_{16})} x_1 x_6$
$x_{10} = \frac{k_{12} (k_{10} + k_{11}) (k_{20} k_{22} x_6 + (k_{21} + k_{22}) (k_{23} + k_{31}))}{r(x_4, x_6)}$	$x_{18} = \frac{k_9 k_{12} (k_{20} k_{22} x_6 + (k_{21} + k_{22}) (k_{23} + k_{31}))}{r(x_4, x_6)} x_4$
$x_{11} = \frac{k_{12} k_{30} (k_{10} + k_{11}) (k_{21} + k_{22})}{r(x_4, x_6)}$	$x_{19} = \frac{k_{12} k_{20} k_{30} (k_{10} + k_{11})}{r(x_4, x_6)} x_6$

This map φ_Y is substituted into (2), and then we saturate. The resulting ideal J_Y equals

$$\langle \alpha_1 x_6 x_8 + \alpha_2 x_4 + \alpha_3 x_6, \quad \alpha_4 x_1 x_6 + \alpha_5 x_1 + \alpha_6 x_8 + \alpha_7, \\ \alpha_8 x_1 x_4 + \alpha_9 x_8 + \alpha_{10}, \quad \alpha_{11} x_4 x_6 x_{13} + \alpha_{12} x_4 x_{13} + \alpha_{13} x_6 x_{13} + \alpha_{14} x_{13} + \alpha_{15}, \\ \alpha_{16} x_4 x_6^2 + \alpha_{17} x_6^3 + \alpha_{18} x_4 x_6 + \alpha_{19} x_6^2 + \alpha_{20} x_8^2 + \alpha_{21} x_1 + \alpha_{22} x_4 + \alpha_{23} x_6 + \alpha_{24} x_8 + \alpha_{25} \rangle,$$

where the $\alpha_1, \dots, \alpha_{25}$ are certain explicit rational functions in the \mathbf{k} -parameters.

6. POLYHEDRAL GEOMETRY

Dynamics of the system while not at steady state cannot typically be studied with algebraic methods. One exception is the set of all possible states accessible from a given set of initial values via the chemical reactions in the model. This set is called a *stoichiometric compatibility class* in the biochemistry literature. Mathematically, these classes are convex polyhedra. We determine them all for the Wnt shuttle model. This resolves Problem 6 from the Introduction.

The conservation relations (2) define a linear map χ from the orthant of concentrations $\mathbb{R}_{\geq 0}^{19}$ to the orthant of conserved quantities $\mathbb{R}_{\geq 0}^5$. We express this projection as a 5×19 -matrix:

$$(7) \quad \begin{pmatrix} c_1 \\ c_2 \\ c_3 \\ c_4 \\ c_5 \end{pmatrix} = \begin{pmatrix} 1 & 1 & 1 & \cdot & \cdot & \cdot & \cdot & \cdot & \cdot & \cdot & \cdot & \cdot & \cdot & \cdot & \cdot & \cdot & \cdot & \cdot & \cdot \\ \cdot & \cdot & \cdot & 1 & 1 & 1 & 1 & \cdot & \cdot & \cdot & \cdot & \cdot & \cdot & \cdot & \cdot & \cdot & \cdot & \cdot & \cdot \\ \cdot & \cdot & \cdot & \cdot & \cdot & \cdot & \cdot & 1 & \cdot & \cdot & \cdot & \cdot & \cdot & \cdot & \cdot & \cdot & \cdot & \cdot & \cdot \\ \cdot & \cdot & \cdot & \cdot & \cdot & \cdot & \cdot & \cdot & 1 & \cdot & \cdot & \cdot & \cdot & \cdot & \cdot & \cdot & \cdot & \cdot & \cdot \\ \cdot & \cdot & \cdot & \cdot & \cdot & \cdot & \cdot & \cdot & \cdot & \cdot & 1 & 1 & \cdot & \cdot & \cdot & \cdot & \cdot & \cdot & \cdot \end{pmatrix} \cdot \begin{pmatrix} x_1 \\ x_2 \\ x_3 \\ \vdots \\ x_{18} \\ x_{19} \end{pmatrix}$$

Let $P_{\mathbf{c}}$ denote the fiber of the map χ for $\mathbf{c} \in \mathbb{R}_{\geq 0}^5$. This is known in the biochemical literature as the *invariant polyhedron* or the *stoichiometric compatibility class* of the given \mathbf{x} ; see e.g. [25, (3)]. The fiber over the origin is $P_{\mathbf{0}} = \mathbb{R}_{\geq 0}\{\mathbf{e}_{10}, \mathbf{e}_{11}\}$, the two-dimensional orthant formed by all positive linear combinations of \mathbf{e}_{10} and \mathbf{e}_{11} . If $\mathbf{c} \in \mathbb{R}_{\geq 0}^5$ is an interior point, then $P_{\mathbf{c}}$ is a 14-dimensional convex polyhedron of the form $P_{\mathbf{0}} \times \tilde{P}_{\mathbf{c}}$ where $\tilde{P}_{\mathbf{c}}$ is a 12-dimensional (compact) polytope. Two vectors \mathbf{c} and \mathbf{c}' are considered *equivalent* if their invariant polyhedra $P_{\mathbf{c}}$ and $P_{\mathbf{c}'}$ have the same normal fan. This property is much stronger than being combinatorially isomorphic. The equivalence classes are relatively open polyhedral cones, and they define a partition of $\mathbb{R}_{\geq 0}^5$. This partition is the *chamber complex* of the matrix (7). For a low-dimensional illustration, see [25, Figure 1]. Informally speaking, the chamber complex classifies the possible boundary behaviors of our dynamical system.

Proposition 6.1. *The chamber complex of our 5×19 -matrix divides $\mathbb{R}_{\geq 0}^5$ into 19 maximal cones. It is the product of a ray, $\mathbb{R}_{\geq 0}$, and the cone over a subdivision of the tetrahedron. That subdivision consists of 18 smaller tetrahedra and 1 bipyramid, described in detail below.*

Proof. The product structure arises because the matrix has two blocks after permuting columns, an upper left 4×17 block and a lower right 1×2 block (1 1). Our task is to compute the chamber decomposition of $\mathbb{R}_{\geq 0}^4$ defined by the 4×17 -block. After deleting zero columns

and multiple columns, we are left with a 4×7 -matrix, given by the seven left columns in

$$M = \begin{pmatrix} a & b & c & d & e & f & g & h & i & j & k & l \\ 0 & 1 & 0 & 0 & 1 & 0 & 0 & 0 & 1 & 1 & 1 & 1 \\ 1 & 1 & 1 & 1 & 0 & 0 & 0 & 1 & 1 & 1 & 1 & 2 \\ 0 & 0 & 1 & 0 & 0 & 1 & 0 & 1 & 0 & 1 & 1 & 1 \\ 0 & 0 & 0 & 1 & 0 & 0 & 1 & 1 & 1 & 0 & 1 & 1 \end{pmatrix}.$$

The correspondence between the seven left columns of M and the columns of (7) is as follows:

$$\begin{aligned} a &= \{x_4, x_5, x_6, x_7, x_{18}, x_{19}\}, & b &= \{x_{14}, x_{15}\}, & c &= \{x_{16}\}, \\ d &= \{x_{17}\}, & e &= \{x_1, x_2, x_3\}, & f &= \{x_8\}, & g &= \{x_9\}. \end{aligned}$$

The remaining columns of M are additional vertices in the subdivision.

The following table lists the 19 maximal chambers. For each chamber we list the extreme rays and the facet-defining inequalities. For instance, the chamber in $\mathbb{R}_{\geq 0}^5$ denoted by $efjk$ is the orthant spanned by the columns e , f , j and k of the matrix M times the ray $(0, 0, 0, 0, 1)^T$. It is defined by $c_5 \geq 0$ together with the four listed inequalities: $c_4 \geq 0$, $\min(c_1, c_3) \geq c_2 \geq c_4$.

$abcd$	$\{c_4, c_3, c_1, c_2 - c_4 - c_3 - c_1\}$
$bcdl$	$\{c_2 - c_3 - c_1, c_2 - c_4 - c_1, c_2 - c_4 - c_3, -c_2 + c_4 + c_3 + c_1\}$
$efgk$	$\{c_2, -c_2 + c_4, -c_2 + c_3, -c_2 + c_1\}$
$bcjl$	$\{c_4, -c_2 + c_1 + c_3, c_2 - c_3 - c_4, c_2 - c_1 - c_4\}$
$bdil$	$\{c_3, -c_2 + c_4 + c_1, c_2 - c_4 - c_3, c_2 - c_3 - c_1\}$
$beij$	$\{c_3, c_4, c_1 - c_2, c_2 - c_3 - c_4\}$
$cdhl$	$\{c_1, -c_2 + c_3 + c_4, c_2 - c_4 - c_3, c_2 - c_4 - c_1\}$
$cfhj$	$\{c_4, c_1, -c_2 + c_3, c_2 - c_4 - c_1\}$
$dghi$	$\{c_1, c_3, -c_2 + c_4, c_2 - c_1 - c_3\}$
$egik$	$\{c_3, -c_2 + c_4, c_2 - c_3, -c_2 + c_1\}$
$fghk$	$\{c_1, -c_1 + c_2, -c_2 + c_3, -c_2 + c_4\}$
$efjk$	$\{c_4, c_1 - c_2, c_2 - c_4, -c_2 + c_3\}$
$bijl$	$\{c_2 - c_1, -c_2 + c_1 + c_3, -c_2 + c_4 + c_1, c_2 - c_3 - c_4\}$
$chjl$	$\{c_2 - c_3, -c_2 + c_4 + c_3, -c_2 + c_3 + c_1, c_2 - c_4 - c_1\}$
$dhil$	$\{c_2 - c_4, -c_2 + c_4 + c_1, -c_2 + c_3 + c_4, c_2 - c_1 - c_3\}$
$ghik$	$\{c_4 - c_2, c_2 - c_3, c_2 - c_1, -c_2 + c_1 + c_3\}$
$eijk$	$\{c_2 - c_4, c_2 - c_3, c_1 - c_2, -c_2 + c_3 + c_4\}$
$fhjk$	$\{c_2 - c_4, c_2 - c_1, -c_2 + c_3, -c_2 + c_4 + c_1\}$
$hijkl$	$\{c_2 - c_4, c_2 - c_3, c_2 - c_1, -c_2 + c_4 + c_3, -c_2 + c_4 + c_1, -c_2 + c_3 + c_1\}$

Interpreting the columns of M as homogeneous coordinates, the table describes a subdivision of the standard tetrahedron into 18 tetrahedra and one bipyramid $hijkl$. These cells use the 12 vertices a, b, \dots, l . The reader is invited to check that this subdivision has precisely 39 edges and 47 triangles, so the Euler characteristic is correct: $12 - 39 + 47 - 19 = 1$. \square

We shall prove the following result about the Wnt shuttle model.

Proposition 6.2. *Suppose that the rate constants k_i and the conserved quantities c_j are all strictly positive. Then no steady states exist on the boundary of the invariant polyhedron P_c .*

Proof. Consider the two components I_m and I_e of the steady state ideal I given in Lemma 3.1. We intersect each of the two varieties with the affine-linear space defined by the conservation relations (2) for some $\mathbf{c} \in \mathbb{R}_{>0}^5$. We claim that all solutions \mathbf{x} satisfy $x_i \neq 0$ for $i = 1, 2, \dots, 19$.

For the main component $V(I_m)$, we prove this assertion with the help of the parametrization φ_Y from Example 5.5. If the values of $x_1, x_4, x_6, x_8, x_{13}$ and of the expression $r(x_4, x_6)$ are nonzero, then each coordinate of φ_Y is nonzero. We next observe that $r(x_4, x_6) > 0$ for any $\mathbf{k} > 0$ and $\mathbf{x} \geq 0$. A case analysis, using binomial relations in the ideal I_m , reveals that if any of $x_1, x_4, x_6, x_8, x_{13}$ are zero, some coordinate of \mathbf{c} is forced to zero as well:

$$\begin{array}{lll}
x_1 = 0 \Rightarrow & x_2, x_3, x_{14}, x_{15} = 0 \Rightarrow & c_1 = 0, \\
x_{13} = 0 \Rightarrow & x_{12} = 0 \Rightarrow & c_5 = 0, \\
x_4 = 0 \Rightarrow & x_5, x_6, x_7, x_{14}, x_{15}, x_{16}, x_{17}, x_{18}, x_{19} = 0 \Rightarrow & c_2 = 0, \\
& \text{or} & x_8, x_{16} = 0 \Rightarrow c_3 = 0, \\
x_6 = 0 \Rightarrow & x_9, x_{17} = 0 \Rightarrow & c_4 = 0, \\
& \text{or} & x_4 = 0 \Rightarrow c_2 \text{ or } c_3 = 0, \\
x_8 = 0 \Rightarrow & x_{16} = 0 \Rightarrow & c_3 = 0.
\end{array}$$

It remains to consider the extinction component. Its ideal I_e contains the set $b \cup l = \{x_1, x_2, x_3, x_{14}, x_{15}\}$. The corresponding columns of the matrix in (7) are the only columns with a nonzero entry in the fourth row. This implies that $c_4 = 0$ holds for every steady state in $V(I_e)$. We conclude that there are no steady states on the boundary of the polyhedron $P_{\mathbf{c}}$. \square

Remark 6.3. In this proof we did not need the detailed description of the chamber complex, because of the special combinatorial structure in the Wnt shuttle model. In general, when studying chemical reaction networks that arise in systems biology, an analysis like Proposition 6.1 is requisite for gaining information about possible zero coordinates in the steady states.

7. PARAMETER ESTIMATION

Question 7 asks: *What information does species concentration data give us for parameter estimation?* This question is of particular importance to experimentalists, as species concentrations depend on initial conditions, whereas parameter values are intrinsic to the biological process being modeled. Identifiability of parameters has been studied in many contexts, notably in statistics [8] and in biological modeling [19]. Sometimes, as in [19], parameters are determined from complete time-course data of the dynamical system, making a differential algebra approach desirable. In the present paper we focus on the steady state variety, so we consider data collection only at steady state. We assume that there is a true but unknown parameter vector $\mathbf{k}^* \in \mathbb{R}^{31}$ of rate constants, and our data are sampled from the positive real points \mathbf{x} on the variety in \mathbb{R}^{19} that is defined by the 19 polynomials in (1).

7.1. Complete Species Information. The first algebraic question we answer: To what extent is the true parameter vector \mathbf{k}^* determined by points on its steady state variety?

To address this question, we form the polynomial matrix $F(\mathbf{x})$ of format 19×31 whose entries are the coefficients of the right-hand sides of (1), regarded as linear forms in \mathbf{k} . With this notation, our dynamical system (1) can be written in matrix-vector product form as

$$\dot{\mathbf{x}} = F(\mathbf{x}) \cdot \mathbf{k}.$$

Our data points are sampled from

$$(8) \quad \{ \mathbf{x} \in \mathbb{R}_{>0}^{19} : F(\mathbf{x}) \cdot \mathbf{k}^* = \mathbf{0} \}.$$

Let $\mathbf{x}_1, \mathbf{x}_2, \mathbf{x}_3, \dots$ denote generic data points in (8). The set of all parameter vectors \mathbf{k} that are compatible with these data is a linear subspace of \mathbb{R}^{31} , namely it is the intersection

$$(9) \quad \text{kernel}(F(\mathbf{x}_1)) \cap \text{kernel}(F(\mathbf{x}_2)) \cap \text{kernel}(F(\mathbf{x}_3)) \cap \dots$$

The best we can hope to recover from sampling data is the following subspace containing \mathbf{k}^* :

$$(10) \quad \bigcap_{\mathbf{x} \text{ in } (8)} \text{kernel}(F(\mathbf{x})) \subset \mathbb{R}^{31}.$$

We refer to (10) as the *space of parameters compatible with \mathbf{k}^** . A direct computation reveals:

Proposition 7.1. *The space of all parameters compatible with \mathbf{k}^* is a 14-dimensional subspace of \mathbb{R}^{31} . If \mathbf{x} is generic then the kernel of $F(\mathbf{x})$ is a 17-dimensional subspace of \mathbb{R}^{31} .*

This has the following noteworthy consequence for our biological application:

Corollary 7.2. *The parameters of the Wnt shuttle model are not identifiable from steady state data, but there are 14 degrees of freedom in recovering the true parameter vector \mathbf{k}^* .*

Our next step is to gain a more precise understanding of the subspaces in Proposition 7.1. To do this, we shall return to the combinatorial setting of matroid theory. We introduce two matroids on the 31 reactions in Table 2. The common ground set is $K = \{k_1, k_2, \dots, k_{31}\}$. The *one-point matroid* \mathcal{M}_{one} is the rank 17 matroid on K defined by the linear subspace $\text{kernel}(F(\mathbf{x}))$ of \mathbb{R}^{31} where $\mathbf{x} \in \mathbb{R}^{19}$ is generic. The *parameter matroid* \mathcal{M}_{par} is the rank 14 matroid on K defined by the space (10) of all parameters compatible with a generic \mathbf{k}^* . The following result, obtained by calculations, reflects the block structure of the matrix $F(\mathbf{x})$.

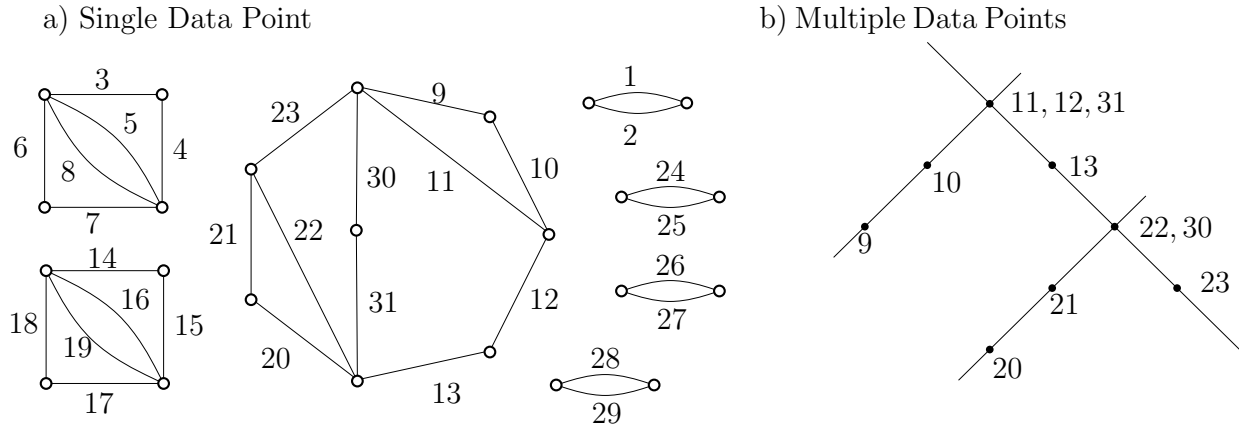


FIGURE 1. Graphic representation of the one-point matroid \mathcal{M}_{one} of rank 17. The rank 4 component of the rank 14 parameter matroid \mathcal{M}_{par} is not graphic.

Proposition 7.3. *The one-point matroid \mathcal{M}_{one} is the graphic matroid of the graph shown in Figure 1 a). Its seven connected components are matroids of ranks 3, 3, 7, 1, 1, 1, 1. The rank 14 parameter matroid \mathcal{M}_{par} is obtained from \mathcal{M}_{one} by specializing the rank 7 component to the rank 4 matroid on 11 elements whose affine representation is shown in Figure 1 b).*

This characterizes the combinatorial constraints imposed on the parameters \mathbf{k} by measuring the species concentrations at steady state. For a single measurement \mathbf{x} , the result on \mathcal{M}_{one} tells us that the 19×31 -matrix $F(\mathbf{x})$ has rank $14 = 31 - \text{rank}(\mathcal{M}_{\text{one}})$. After row operations, it block-decomposes into two matrices of format 3×6 , one matrix of format 4×11 , and four matrices of format 1×2 . Each of these seven matrices is row-equivalent to the node-edge *cycle matrix* of a directed graph, with underlying undirected graph as in Figure 1 (a).

Consider the graph with edges 9, 10, 11, 12, 13, 20, 21, 22, 23, 30, 31. The cycle $\{22, 23, 30, 31\}$ reveals that our measurement \mathbf{x} imposes one linear constraint on $k_{22}, k_{23}, k_{30}, k_{31}$. If we take further measurements, as in (9), then six of the seven blocks of $F(\mathbf{x})$ remain unchanged. Only the 4×11 -block of $F(\mathbf{x})$ must be enlarged, to a 7×11 -matrix. The rows of that new matrix specify the affine-linear dependencies among 11 points in \mathbb{R}^3 . That point configuration is depicted in Figure 1 (b). For instance, the points $\{9, 10, 11\}$ are collinear, the points $\{20, 21, 22\}$ are collinear, but these two lines are skew in \mathbb{R}^3 . From the other line we see that that repeated measurements at steady state impose two linear constraints on $k_{22}, k_{23}, k_{30}, k_{31}$.

7.2. Circuit Data. The second question we address in this section: *Given partial species concentration data, is any information about parameters available?* In Section 7.1, all 19 concentrations x_i were available for a steady state. In what follows, we suppose that x_i can only be measured for indices i in a subset of the species, say $C \subset \{1, \dots, 19\}$. In our analysis, it will be useful to take advantage of the rank 5 algebraic matroid in Proposition 5.2, since that matroid governs dependencies among the coordinates x_1, \dots, x_{19} at steady states.

We here focus on the special case when C is one of the 951 circuits of the algebraic matroid of \widetilde{I}_m . Let f_C be the corresponding circuit polynomial, as in Table 5. We regard f_C as a polynomial in \mathbf{x} whose coefficients are polynomials in $\mathbb{Q}[\mathbf{k}]$. Suppose that f_C has r monomials $\mathbf{x}^{a_1}, \dots, \mathbf{x}^{a_r}$. We write $F_C \in \mathbb{Q}[\mathbf{k}]^r$ for the vector of coefficients, so our circuit polynomial is the dot product $f_C(\mathbf{k}, \mathbf{x}) = F_C(\mathbf{k}) \cdot (\mathbf{x}^{a_1}, \dots, \mathbf{x}^{a_r})$. We write $\mathcal{V}_C \subset \mathbb{R}^r$ for the algebraic variety parametrized by $F_C(\mathbf{k})$. Thus \mathcal{V}_C is the Zariski closure in \mathbb{R}^r of the set $\{F_C(\mathbf{k}') : \mathbf{k}' \in \mathbb{R}^{31}\}$.

Our idea for parameter recovery is this: rather than looking for \mathbf{k} compatible with the true parameter \mathbf{k}^* , we seek a point $\mathbf{y} = F_C(\mathbf{k})$ in \mathcal{V}_C that is compatible with $F_C(\mathbf{k}^*)$. And, only later do we compute a preimage of \mathbf{y} under the map $\mathbb{R}^{31} \rightarrow \mathbb{R}^r$ given by F_C . Most interesting is the case when \mathcal{V}_C is a proper subvariety of \mathbb{R}^r . Direct computations yield the following:

Proposition 7.4. *For precisely 288 of the 951 circuits C of the algebraic matroid of the steady state ideal \widetilde{I}_m , the coefficient variety \mathcal{V}_C is a proper subvariety in its ambient space \mathbb{R}^r . In each of these cases, the defining ideal of \mathcal{V}_C is of one of the following four types:*

$$(11) \quad \langle y_2 y_6 - y_3 y_5 \rangle$$

$$(12) \quad \langle y_5 y_6 - 2y_3 y_7, y_5^2 - 4y_2 y_7, y_3 y_5 - 2y_2 y_6, y_2 y_6^2 - y_3^2 y_7 \rangle$$

$$(13) \quad \langle y_3 y_5^2 - y_2 y_5 y_6 + y_1 y_6^2 \rangle$$

$$(14) \quad \langle 2y_3 y_4 - y_2 y_5, y_2 y_3 - 2y_1 y_5, y_2^2 - 4y_1 y_4 \rangle$$

Example 7.5. Consider the circuit $C = \{6, 10, 18\}$. The circuit polynomial f_C equals

$$\begin{aligned} & (k_{13}k_{20}k_{22} + k_{20}k_{22}k_{30}) \cdot x_6x_{10} + k_{11}k_{20}k_{22} \cdot x_6x_{18} - k_{12}k_{20}k_{22} \cdot x_6 \\ & + (k_{13}k_{21}k_{23} + k_{13}k_{22}k_{23} + k_{21}k_{23}k_{30} + k_{22}k_{23}k_{30} + k_{13}k_{21}k_{31} + k_{13}k_{22}k_{31}) \cdot x_{10} \\ & + (k_{11}k_{21}k_{23} + k_{11}k_{22}k_{23} + k_{11}k_{21}k_{31} + k_{11}k_{22}k_{31}) \cdot x_{18} \\ & - (k_{12}k_{21}k_{23} + k_{12}k_{22}k_{23} + k_{12}k_{21}k_{31} + k_{12}k_{22}k_{31}). \end{aligned}$$

Here $r = 6$ and we write $F_C(\mathbf{k}) = (y_1, y_2, y_3, y_4, y_5, y_6)$ for the vector of coefficient polynomials. The variety \mathcal{V}_C is the hypersurface in \mathbb{R}^5 defined by the equation $y_2y_6 = y_3y_5$.

We now sample data points \mathbf{x}_i from the model with the true (but unknown) parameter vector \mathbf{k}^* . Each such point defines a hyperplane $\{\mathbf{y} \in \mathbb{R}^r : \mathbf{y} \cdot (\mathbf{x}_1^{a_1}, \dots, \mathbf{x}_r^{a_r}) = 0\}$. The parameter estimation problem is to find the intersection of these data hyperplanes with the variety \mathcal{V}_C . That intersection contains the point $\mathbf{y}^* = F_C(\mathbf{k}^*)$, which is what we now aim to recover.

7.3. Noisy Circuit Data. The final question we consider in this section is: *Given partial species concentration data with noise, is any information about parameters available?*

As in Section 7.2, we fix a circuit C of the algebraic matroid in Section 5, and we assume that we can only measure the concentrations x_j where $j \in C$. Each measurement $\mathbf{x}_i \in \mathbb{R}^C$ still defines a hyperplane $\mathbf{y} \cdot (\mathbf{x}_i^{a_1}, \dots, \mathbf{x}_i^{a_r}) = 0$ in the space \mathbb{R}^r . But now the true vector $\mathbf{y}^* = F_C(\mathbf{k}^*)$ is not exactly on that hyperplane, but only close to it. Hence, if we take s repeated measurements, with $s > r$, the intersection of these hyperplanes should be empty.

We propose to find the best fit by solving the following least squares optimization problem:

$$(15) \quad \text{Minimize} \quad \sum_{i=1}^s (\mathbf{y} \cdot (\mathbf{x}_i^{a_1}, \dots, \mathbf{x}_i^{a_r}))^2 \quad \text{subject to} \quad \mathbf{y} \in \mathcal{V}_C \cap \mathbb{S}^{r-1},$$

where $\mathbb{S}^{r-1} = \{\mathbf{y} \in \mathbb{R}^r : y_1^2 + y_2^2 + \dots + y_r^2 = 1\}$ denotes the unit sphere. When the variety \mathcal{V}_C is the full ambient space \mathbb{R}^r , this is a familiar regression problem, namely, to find the hyperplane through the origin that best approximates s given points in \mathbb{R}^r . Here “best” means that the sum of the squared distances of the s points to the hyperplane is minimized. This happens for 663 of the 951 circuits C , and in that case we can apply standard techniques.

However, for the 288 circuits C identified in Proposition 7.4, the problem is more interesting. Here the hyperplanes under consideration are constrained to live in a proper subvariety. In that case we need some algebraic geometry to reliably find the global optimum in (15).

Our problem is to minimize a quadratic function over the real affine variety $\mathcal{V}_C \cap \mathbb{S}^{r-1}$. The quadratic objective function is generic because the \mathbf{x}_i are sampled with noise. The intrinsic algebraic complexity of our optimization problem was studied by Draisma et al. in [5]. That complexity measure is the *ED degree* of $\mathcal{V}_C \cap \mathbb{S}^{r-1}$, which is the number of solutions in \mathbb{C}^r to the critical equations of (15). Here, by ED degree we mean the ED degree of $\mathcal{V}_C \cap \mathbb{S}^{r-1}$, when considered in generic coordinates. This was called the *generic ED degree* in [20].

We illustrate our algebraic approach by working out the first instance (11) in Proposition 7.4.

Example 7.6. Suppose we are given s noisy measurements of the concentrations x_6, x_{10}, x_{18} . In order to find the best fit for the parameters \mathbf{k} , we employ the circuit polynomial f_C in

Example 7.5. We compute $\mathbf{y} \in \mathbb{R}^6$ by solving the corresponding optimization problem (16). This problem is to minimize a random quadratic form subject to two quadratic constraints

$$(16) \quad y_2 y_6 - y_3 y_5 = y_1^2 + y_2^2 + y_3^2 + y_4^2 + y_5^2 + y_6^2 - 1 = 0.$$

We solve this problem using the method of Lagrange multipliers. This leads to a system of polynomial equations in \mathbf{y} . Using saturation, we remove the singular locus of (16), which is the circle $\{\mathbf{y} \in \mathbb{R}^6 : y_1^2 + y_4^2 - 1 = y_2 = y_3 = y_5 = y_6 = 0\}$. The resulting ideal has precisely 40 zeros in \mathbb{C}^6 . In the language of [5, 20], the generic ED degree of the variety (16) equals 40.

8. FROM ALGEBRA TO BIOLOGY

The aims of this paper are: (1) to demonstrate how biology can lead to interesting questions in algebraic geometry, and (2) to apply new techniques from computational algebra in biology. So far, our tour through (numerical) algebraic geometry, polyhedral geometry and combinatorics has demonstrated the range of mathematical questions to explore. In this section, we will focus on translating our analysis into applicable considerations for the research cycle in systems biology, which is illustrated in Figure 2. In what follows we discuss some concrete applications and results pertaining to the steps (a), (b) and (c) in Figure 2.

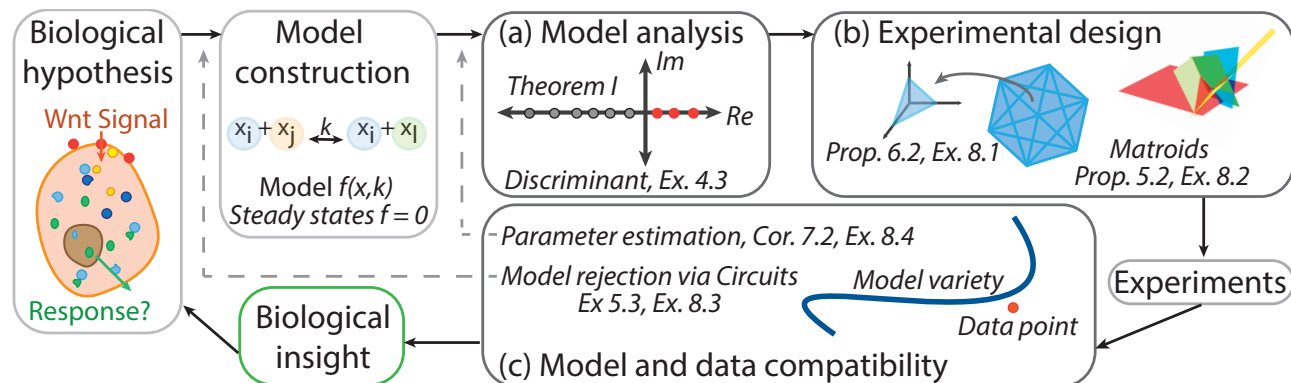


FIGURE 2. Systems biology cycle informed by algebraic geometry and combinatorics. (a) Model analysis. See Sections 1, 3, 4. (b) Experimental design. See Sections 5 and 6. (c) Model and data compatibility. See Sections 5 and 7.

Analysis of the Model: Before any experiments are performed, our techniques inform the modeler of the global steady-state properties of the model. The number of real solutions to system (1)–(2), stated in Theorem 1.1, governs the number of observable steady states. Various sampling schemes demonstrated that *most* parameter values lead to only one observable steady state. We produced a set of parameter values and conserved quantities with three real solutions, and two solutions are also attainable. If the “true” parameters \mathbf{k}^* and \mathbf{c}^* admit multiple real solutions, then multistationarity of the system is theoretically possible.

If multiple states are observed experimentally, then the model must be capable of multistationarity. In the Wnt shuttle model, the system is capable of multiple steady states; however, based on parameter sampling, the frequency of this occurrence is low, and parameters in this

regime are somewhat stable under perturbation. The discriminant of the system is a polynomial of degree 34 in \mathbf{c} , and our analysis along a single line in \mathbf{c} -space illustrates the high degree of complexity inherent in the full stratification of the 36-dimensional parameter space.

Experimental Design: In Section 6, the combinatorial structure of the various stoichiometric compatibility classes was fully characterized. As the conserved quantities $\mathbf{c} = (c_1, \dots, c_5)$ range over all positive real values, the set of all compatible species-concentration vectors \mathbf{x} will take one of 19 polyhedral shapes $P_{\mathbf{c}}$. This may find application in identifying multiple steady state solutions for specific rate constants \mathbf{k} . A natural choice for initial conditions when performing experiments is on or near the vertices of the 14-dimensional polyhedron $P_{\mathbf{c}}$.

Example 8.1. Suppose the conserved quantities vector lies in the bipyramid, e.g. $\mathbf{c} = (1, 2, 2, 2, 3)$. The preimage of \mathbf{c} in \mathbf{x} -space is a product of the orthant $\mathbb{R}_{\geq 0}\{\mathbf{e}_{10}, \mathbf{e}_{11}\}$ and a 12-dimensional polytope with 400 vertices: $(1, 0, 0, 2, 0, 0, 0, 2, 2, 0, 0, 3, 0, 0, 0, 0, 0, 0, 0)$, and 399 of its permutations. This product is the polyhedron $P_{\mathbf{c}}$. If we have control over initial conditions, beginning near the vertices positions us to find interesting systems behavior.

In the laboratory, the experimentalist makes choices of what to measure and what not to measure. For instance, measuring a particular x_i may be infeasible, or there may be a situation in which measuring concentration x_i can preclude measuring concentration x_j .

For every strategy, we fix a *cost vector*, listing the costs of making each measurement. We use the symbol N to indicate infeasible measurements. Suppose there are two different ways to run the experiment; then we have a 2×19 *cost matrix* P , whose rows are cost vectors for each experiment. We multiply P by the 0-1-incidence matrix for the 951 circuits of Proposition 5.2. That matrix has a 1 in row i and column j if circuit j contains species i , and 0 otherwise. The product is a matrix of size 2×951 . For $N \rightarrow \infty$, the 2×951 matrix has a finite entry in position (i, j) precisely when the strategy i can measure the circuit j . Minimizing over those finite cost entries selects the most cost-effective experiment to measure a circuit.

Example 8.2. Suppose that none of the intermediate complexes x_{13}, \dots, x_{19} are measurable, and that we are able to measure only one Phosphatase concentration (x_4 or x_8) in each experimental setup. A corresponding cost matrix might look like

$$P = \begin{bmatrix} 1 & 1 & 1 & N & 1 & 1 & 1 & 1 & 1 & 1 & 1 & 1 & N & N & N & N & N & N & N \\ 1 & 1 & 1 & 1 & 1 & 1 & 1 & N & 1 & 1 & 1 & 1 & N & N & N & N & N & N & N \end{bmatrix}$$

Multiplying by the circuit support matrix of size 19×951 reveals 82 feasible experiments: 50 using the first row of P , and 32 using the second. With more refined cost assignment, this would decide not only feasibility but also optimal cost. In this way, the matroid allows us to choose cost-minimal experiments to obtain meaningful information for the model.

Model and data compatibility: After an experiment is performed, the task of the modeler is to test the data with the model. One possible outcome is *model rejection*. If the data are compatible, then another outcome is *parameter estimation*. Both may provide insights for biology. The role of algebraic geometry is seen in [9, 10] and shown in the next two examples.

Example 8.3 (Model Rejection). Suppose that rate parameters k_i are all known to be 1, and that we have collected data for variables x_1, x_4, x_{14} . The circuit polynomial is $k_1 k_3 x_1 x_4 + (-k_2 k_4 - k_2 k_5) x_{14}$, which specializes to $x_1 x_4 - 2x_{14}$. If the evaluation of the positive quantity $|x_1 x_4 - 2x_{14}|$ lies above a threshold ϵ , then we can reject the model as not matching the data.

Every circuit polynomial of the matroid is a *steady state invariant*; depending on which experiment was performed, the collection of measured variables must contain some circuit. Even if one can measure all 19 species at steady state, it is not possible to recover all 31 kinetic rate constants, but we do have relationships that must be satisfied among parameters [16].

Example 8.4 (Parameter Estimation). Suppose that rate parameters are unknown, and that we have collected data for x_6, x_{10}, x_{18} . The corresponding circuit polynomial f_C is shown in Example 7.5. We know that the coefficients of f_C satisfy the constraint $y_2y_6 = y_3y_5$. Suppose our experiments lead to the following ten measurements for the vector (x_6, x_{10}, x_{18}) :

$$\begin{aligned} & \{(.715335, 4.06778, 14.6806), (.390982, 4.83152, 6.08251), (.706539, 4.98107, 3.83617), \\ & (.14316, 4.30851, 12.5809), (.995583, 4.01222, 15), (.413817, 4.08114, 14.902), (.232206, 3.38274, 23.3162), \\ & (.219045, 5.06008, 3.67175), (.704106, 3.52804, 21.1037), (.648732, 3.6505, 19.7008)\} \end{aligned}$$

The data lead us to the following function to optimize in (15):

$$\begin{aligned} & 57.2345y_1^2 + 376.181y_1y_2 + 801.672y_2^2 - 27.5625y_1y_3 - 96.4429y_2y_3 \\ & + 3.36521y_3^2 + 179.49y_1y_4 + 564.034y_2y_4 - 42.729y_3y_4 + 178.839y_4^2 + 564.034y_1y_5 \\ & + 2424.31y_2y_5 - 144.7y_3y_5 + 1054.49y_4y_5 + 2263.2y_5^2 - 42.729y_1y_6 \\ & - 144.7y_2y_6 + 10.339y_3y_6 - 83.8072y_4y_6 - 269.749y_5y_6 + 10y_6^2 \end{aligned}$$

The global minimum of this quadratic form on the codimension 2 variety (16) has coordinates

$$y_1 = 0.183472, y_2 = 0.152416, y_3 = 0.959232, y_4 = 0.038042, y_5 = 0.00335267, y_6 = 0.211.$$

Given these values, one now has three degrees of freedom in estimating the nine parameters k_i that appear in the circuit polynomial f_C . The other ten coordinates of \mathbf{k} are unspecified.

ACKNOWLEDGEMENTS

This project was supported by UK Royal Society International Exchange Award 2014/R1 IE140219. EG, BS and HAH initiated discussions at an American Institute of Mathematics workshop in Palo Alto. Part of the work was carried out at the Simons Institute for Theory of Computing in Berkeley. HAH gratefully acknowledges EPSRC Fellowship EP/K041096/1. EG, ZR and BS were also supported by the US National Science Foundation, through grants DMS-1304167, DMS-0943745 and DMS-1419018 respectively. Thanks to Helen Byrne and Reinhard Laubenbacher for comments on early drafts of the paper.

REFERENCES

- [1] D. Bates, J. Hauenstein, A. Sommese and C. Wampler: *Numerically Solving Polynomial Systems with Bertini*, Software, Environments, and Tools, Vol. 25, SIAM, Philadelphia, 2013.
- [2] D. Bates, E. Gross, A. Leykin and J. Rodriguez: *Bertini for Macaulay2*, [arXiv:1310.3297](https://arxiv.org/abs/1310.3297).
- [3] C. Chen, J. Davenport, M. Moreno Maza, B. Xia and R. Xiao: Computing with semi-algebraic sets: Relaxation techniques and effective boundaries, *J. Symbolic Computation* **52** (2013), 72–96.
- [4] G. Craciun and M. Feinberg: Multiple equilibria in complex chemical reaction networks. I. The injectivity property, *SIAM J. Appl. Math.* **65** (2005) 1526–1546.
- [5] J. Draisma, E. Horobet, G. Ottaviani, B. Sturmfels and R.R. Thomas: The Euclidean distance degree of an algebraic variety, *Foundations of Computational Mathematics*, to appear, [arXiv:1309.0049](https://arxiv.org/abs/1309.0049).

- [6] J-C. Faugère, G. Moroz, F. Rouillier and M. Safey El Din: Classification of the perspective-three-point problem, discriminant variety and real solving polynomial systems of inequalities, *ISSAC 2008*, 79–86, ACM, New York, 2008.
- [7] E. Feliu and C. Wiuf: Variable elimination in chemical reaction networks with mass-action kinetics, *SIAM J. Appl. Math.* **72** (2012) 959–981.
- [8] L. Garcia-Puente, S. Petrovic and S. Sullivant: Graphical models, *J. Softw. Algebra Geom.* **5** (2013) 1–7.
- [9] E. Gross, B. Davis, K. Ho, D. Bates and H. Harrington: Model selection using numerical algebraic geometry, in preparation.
- [10] H. Harrington, K. Ho, T. Thorne and M. Stumpf: Parameter-free model discrimination criterion based on steady-state coplanarity, *Proc. Natl. Acad. Sci.* **109** (2012) 15746–15751.
- [11] D. Grayson and M. Stillman: *Macaulay2, a software system for research in algebraic geometry*, available at www.math.uiuc.edu/Macaulay2/.
- [12] R. Karp, M. Pérez Millán, T. Desgupta, A. Dickenstein and J. Gunawardena: Complex-linear invariants of biochemical networks, *J. Theoret. Biol.* **311** (2012) 130–138.
- [13] E. Klipp, W. Liebermeister, C. Wierling, A. Kowald, H. Lehrach and R. Herwig: *Systems Biology*, John Wiley & Sons, 2009.
- [14] F. Király, Z. Rosen and L. Theran: Algebraic matroids with graph symmetry, [arXiv:1312.3777](https://arxiv.org/abs/1312.3777).
- [15] F. Király, L. Theran, R. Tomioka: The algebraic combinatorial approach for low-rank matrix completion, to appear in *Journal of Machine Learning Research*, [arXiv:1211.4116](https://arxiv.org/abs/1211.4116).
- [16] A. MacLean, H. Harrington, M. Stumpf and H. Byrne: Mathematical and statistical techniques for systems medicine: The Wnt signaling pathway as a case study, in *Systems Biology for Medicine*, to appear the series “Methods in Molecular Biology”, Springer, New York.
- [17] A. MacLean, Z. Rosen, H. Byrne and H. Harrington: Parameter-free methods distinguish Wnt pathway models and guide design of experiments, *Proc. Natl. Acad. Sci.*, to appear, [arXiv:1409.0269](https://arxiv.org/abs/1409.0269).
- [18] N. Meshkat and S. Sullivant: Identifiable reparametrizations of linear compartment models, *J. Symbolic Comput.* **63** (2014) 46–67.
- [19] A. Morgan and A. Sommese: Coefficient-parameter polynomial continuation, *Appl. Math. Comput.* **29** (1989) 123–160.
- [20] G. Ottaviani, P-J. Spaenlehauer and B. Sturmfels: Exact solutions in structured low-rank approximation, *SIAM J. Matrix Anal. Appl.* **35** (2014) 1521–1542.
- [21] J. Oxley: *Matroid Theory*, Oxford University Press, 2011.
- [22] M. Pérez Millán, A. Dickenstein, A. Shiu and C. Conradi: Chemical reaction systems with toric steady states, *Bull. Math. Biol.* **74** (2012) 1027–1065.
- [23] J. Rodriguez and X. Tang: *Data-discriminants of likelihood equations*, [arXiv:1501.00334](https://arxiv.org/abs/1501.00334).
- [24] Z. Rosen: Computing algebraic matroids, [arXiv:1403.8148](https://arxiv.org/abs/1403.8148).
- [25] A. Shiu and B. Sturmfels: Siphons in chemical reaction networks, *Bull. Math. Biol.* **72** (2010) 1448–1463.
- [26] J. Verschelde: Algorithm 795: PHCpack: A general-purpose solver for polynomial systems by homotopy continuation, *ACM Trans. Math. Softw.* **25** (1999) 251–276.
- [27] E. Voit: *A First Course in Systems Biology*, Garland Science, 2012.

ELIZABETH GROSS: SAN JOSÉ STATE UNIVERSITY, elizabeth.gross@sjsu.edu

HEATHER A. HARRINGTON: UNIVERSITY OF OXFORD, harrington@maths.ox.ac.uk

ZVI ROSEN: UNIVERSITY OF CALIFORNIA AT BERKELEY, zhrosen@berkeley.edu

BERND STURMFELS: UNIVERSITY OF CALIFORNIA AT BERKELEY, bernd@berkeley.edu